

See discussions, stats, and author profiles for this publication at: <https://www.researchgate.net/publication/231273427>

# Effects of Temperature on the Formation of Lignin-Derived Oligomers during the Fast Pyrolysis of Mallee Woody Biomass

ARTICLE *in* ENERGY & FUELS · MARCH 2008

Impact Factor: 2.79 · DOI: 10.1021/ef7007634

---

CITATIONS

111

---

READS

31

6 AUTHORS, INCLUDING:



J. Shen

Taiyuan University of Technology

20 PUBLICATIONS 465 CITATIONS

SEE PROFILE



Martin Rhodes

Monash University (Australia)

90 PUBLICATIONS 2,407 CITATIONS

SEE PROFILE

# Effects of Temperature on the Formation of Lignin-Derived Oligomers during the Fast Pyrolysis of Mallee Woody Biomass

Manuel Garcia-Perez,<sup>†,‡</sup> Shan Wang,<sup>†</sup> Jun Shen,<sup>†,§</sup> Martin Rhodes,<sup>†</sup> Woo Jin Lee,<sup>†</sup> and Chun-Zhu Li<sup>\*,†</sup>

Department of Chemical Engineering, PO Box 36, Monash University, Victoria 3800, Australia; Biological Systems Engineering Department, Washington State University, Pullman, Washington 99164; and Department of Chemical Engineering, Taiyuan University of Technology, Shanxi 030024, P. R. China

Received December 16, 2007. Revised Manuscript Received February 7, 2008

This paper reports the evolution of the composition of bio-oil obtained from the fast pyrolysis of Mallee woody biomass as a function of temperature between 350 and 580 °C. Several analytical techniques were used to quantify bio-oil composition. For the volatile components, the results obtained by gas chromatography–mass spectrometry and Karl Fischer titration agree very well with those obtained by thermogravimetric analyses. However, for the heavy components, especially lignin-derived oligomers, synchronous UV-fluorescence spectroscopy and thermogravimetric analysis give more reliable results than the precipitation in cold water. Our results indicate that the accuracy of the precipitation methods to quantify lignin-derived oligomer in bio-oil is limited by the relatively large amounts of small oligomers remaining soluble in a metastable form in cold water. A maximum in the yield of lignin-derived oligomers was observed between 450 and 500 °C. In fact, most of the increases in the yield of bio-oil with increasing temperature above 350 °C can be explained by the formation of this type of oligomers. Increases in the rates at which the oligomers are formed and increases in their volatility at elevated temperature are the main reasons for the increased presence of oligomers in bio-oil produced at temperatures higher than 350 °C.

## 1. Introduction

The growing importance of biofuels is a direct consequence of the recent increases in petroleum price, the increased awareness of the devastating effects of global warming, and the need to spur rural development. Although there are several viable ways to use biomass as an energy source, the production of transportation fuels and high-value chemicals remains the priority for most research efforts, noting that biomass is our only direct abundant renewable source for these products. The production of bio-oil from the pyrolysis of biomass appears particularly attractive. The crude bio-oil produced at the distributed locations may be transported for central processing (biorefinery), representing a new model of biomass economy.

The production of bio-oil from the fast pyrolysis of biomass has been the subject of intensive research for the past three decades.<sup>1–7</sup> It is now firmly established that the maximum yields of bio-oil are obtained at temperatures between 450 and 500

°C at which up to 70 mass % of the biomass can be converted to a crude bio-oil. Many studies on fast pyrolysis have been conducted with the aim to maximize the yield of bio-oil, however, without recognizing that the process conditions for the maximum bio-oil yields may not coincide with those for producing a bio-oil with the best quality.<sup>8</sup> There is therefore a need to consider bio-oil quality requirement taking into account each targeted application.

High molecular mass oligomers are an important part of bio-oil, especially for bio-oils produced at high heating rates. For example, the fast pyrolysis of cellulose and hemicellulose may produce large amounts of anhydro-oligosugars<sup>9–14</sup> that could become an important alternative source for fermentable sugars to produce ethanol. On the other hand, the presence of large amounts of high molecular mass oligomers may not be advantageous if the bio-oil is to be used directly as a liquid fuel. The yield and structure of oligomers in a bio-oil would also be an important consideration if the bio-oil is considered as a feedstock for a biorefinery.

The mechanisms by which lignin-derived oligomers are formed during fast pyrolysis are not well-known,<sup>7</sup> although the

\* To whom correspondence should be addressed. Telephone: +61 3 9905 9623. Fax: +61 3 9905 5686. E-mail: chun-zhu.li@eng.monash.edu.au.

<sup>†</sup> Monash University.

<sup>‡</sup> Washington State University.

<sup>§</sup> Taiyuan University of Technology.

(1) Scott, D. S.; Piskorz, J. *Can. J. Chem. Eng.* **1982**, *60*, 666–674.

(2) Scott, D. S.; Piskorz, J. *Can. J. Chem. Eng.* **1984**, *62*, 291–294.

(3) Scott, D. S.; Piskorz, J.; Radlein, D. *Ind. Eng. Chem. Res.* **1988**, *27*, 8–15.

(4) Scott, D. S.; Majerski, P.; Piskorz, J.; Radlein, D. *J. Anal. Appl. Pyrol.* **1999**, *51*, 23–37.

(5) Agblevor, F. A.; Besler, S. *Energy Fuels* **1996**, *10*, 293–298.

(6) Bridgwater, A. V.; Meier, D.; Radlein, D. *Org. Geochem.* **1999**, *30*, 1479–1493.

(7) Dugaard, D. E.; Brown, R. The transport phase of pyrolytic oil exiting a fluidized bed reactor. In *Proceedings of Science in Thermal and Chemical Biomass Conversion*; Bridgwater, A. V., Boocock, D. G. B., Eds.; CPL Press: Newbury, UK, 2006; 1189–1202.

(8) Kersten, S. R. A.; Wang, X.; Prins, W.; van Swaaij, W. P. M. *Ind. Eng. Chem. Res.* **2005**, *44*, 8773–8785.

(9) Piskorz, J.; Radlein, D.; Scott, D. S. *J. Anal. Appl. Pyrolysis* **1986**, *9*, 121–137.

(10) Piskorz, J.; Majerski, P.; Radlein, D.; Scott, D. S.; Bridgwater, A. V. *J. Anal. Appl. Pyrolysis* **1998**, *46*, 15–29.

(11) Piskorz, J.; Majerski, P.; Radlein, D.; Vladars-Usas, A.; Scott, D. S. *J. Anal. Appl. Pyrolysis* **2000**, *56*, 145–166.

(12) Radlein, D.; Grinshpun, A.; Piskorz, J.; Scott, D. S. *J. Anal. Appl. Pyrolysis* **1987**, *12*, 39–49.

(13) Radlein, D.; Piskorz, J.; Scott, D. S. *J. Anal. Appl. Pyrolysis* **1991**, *19*, 41–63.

(14) Lomax, J. A.; Commandeur, J. M.; Arisz, P. W.; Boon, J. *J. Anal. Appl. Pyrolysis* **1991**, *19*, 65–79.

characterization of lignin-derived oligomers in pyrolysis oil has received considerable attention.<sup>15–19</sup> It has been proved that at least a part of the water-CH<sub>2</sub>Cl<sub>2</sub>-insoluble oligomers (heavy oligomers) found in bio-oil is due to the random condensation of pyrolysis primary products during storage.<sup>20–23</sup> However, there is also considerable evidence that a significant fraction of oligomers is formed inside the pyrolysis reactors.<sup>7</sup> Kawamoto et al.<sup>24</sup> have proven that, in addition to the formation of monomers, several competitive pathways leading to the formation of dimmers were also identified during the pyrolysis of lignin.

Further advances in the understanding of oligomer formation suffer from the lack of suitable analytical techniques to characterize the bio-oil with an exceedingly complex composition. While water and volatile organic compounds can be quantified using gas chromatography (GC), mono- and oligo-sugars and high molecular mass lignin-derived oligomers can also be found in a bio-oil sample but cannot be easily quantified by these methods.<sup>25–27</sup> Consequently, more than one analytical technique has to be used to characterize bio-oil chemical composition. Nondestructive methods would be of clear advantages considering the reactive nature of bio-oil samples.

Solvent extraction techniques have played a very important role in the understanding of bio-oil global chemical composition.<sup>15,21,27</sup> However, all the fractionation strategies have an intrinsic drawback in that, although each class/group of bio-oil compounds tends to be concentrated in one of the used solvents, the distribution coefficients are not high enough to ensure a clear cut of the chemical species among solvents.<sup>27</sup> More than one property, such as molecular mass and the abundance of polar functional groups, could affect the distribution coefficients. Consequently, many chemical compounds can be found in all the solvents used.

Thermogravimetric analyses (TGA) have been proposed<sup>27,28</sup> for quantifying the chemical composition of bio-oil in terms of chemical families. Based on the evaporation or partial decomposition and subsequent evaporation of various components, the TGA analysis of bio-oil showed great promise in classifying the components in bio-oils. Clearly, further study is required to demonstrate the full potential of this novel technique in characterizing bio-oils.

UV-fluorescence spectroscopy has been extensively used for studying the structural features of tar and other coal/biomass-

derived liquids.<sup>29–31</sup> It has proved to be a very useful tool to examine the structural features of the liquid samples. As a nondestructive technique, UV-fluorescence spectroscopy can give information about the relative size and concentration of aromatic ring systems in oligomeric structures. In particular, the constant energy synchronous fluorescence spectroscopy greatly simplifies the analysis of complex mixtures since it takes advantage of the constant and known vibrational spacing for classes of compounds. In spite of its well-known quantitative nature, UV-fluorescence spectroscopy has not been used for quantifying the families of chemical components in bio-oils.

The main purpose of this study was to gain insights into the complex composition of bio-oil produced from the fast pyrolysis of mallee woody biomass. An array of well-accepted analytical techniques, such as gas chromatography–mass spectrometry (GC-MS), Karl Fischer titration, and solvent extraction, and novel approaches, such as TGA and UV-fluorescence spectroscopy, were used to follow the evolution of bio-oil chemical composition as a function of pyrolysis temperature between 350 and 580 °C. Special attention is focused on the quantification of lignin-derived oligomers to shed light on the mechanisms of their formation.

## 2. Experimental Section

**2.1. Biomass Sample.** Mallee woody biomass (*eucalyptus Loxophleba*, subspecies *Lissophloia*) and pine pellets were the feedstocks used for producing the bio-oil samples herein studied. The mallee woody biomass was received in trunks from the Department of Conservation and Lands, Western Australia. The pine pellets tested for comparison purposes were obtained from the Southern Shaving Co, Cherryville, NC. Both materials were ground and sieved to fractions between 90 and 600 μm. A more detailed description of these feedstocks can be found elsewhere.<sup>32</sup>

**2.2. Fast Pyrolysis.** The pyrolysis experiments were conducted using a fluidized-bed pyrolysis reactor with a nominal capacity of 2 kg/h feedstock. Details of this facility are given elsewhere.<sup>32</sup> Briefly, the setup consisted of a sealed hopper, a screw feeder of adjustable speed, a fluidized-bed reactor, cyclones, and condensers. Nitrogen used as the fluidization gas was preheated using an electrical heater. All the tests were carried out at gas velocities 2.3 times the minimum fluidization velocity of the bed solids (washed silica sand). Heating tapes were installed on the walls of the reactor, cyclones, and pipes to supply additional heat and to prevent heat losses. Two cyclones in series were used to collect the char particles. Bio-oil collection was performed in three sequential steps. Gas exit temperature of around −8 °C was achieved in the last condenser. Most of the aerosols were trapped by a 240 mm Advantec quantitative filter paper No. 1 with 65% collection efficiency for particles over 0.3 μm.

**2.3. Bio-oil Characterization.** The water content was determined by Karl Fischer titration (KF DL31 from Mettler-Toledo) using 5-keto as a titrant. The quantification of the content of lignin-derived oligomers in bio-oil was attempted by means of precipitation in cold water, following a method similar to the one detailed elsewhere.<sup>15,27</sup> Briefly, 3 g of bio-oil was added into 300 mL of ice-cooled water dropwise under strong agitation. Preliminary tests with larger samples (more than 4 g) were carried out in an attempt to increase the size of bio-oil samples and consequently reduce the

(15) Sipila, K.; Kuoppale, E.; Fagernas, L.; Oasmaa, A. *Biomass Bioenergy* **1998**, *14* (2), 103–113.

(16) Scholze, B.; Meier, D. *J. Anal. Appl. Pyrolysis* **2001a**, *60*, 41–54.

(17) Scholze, B.; Hanser, C.; Meier, D. *J. Anal. Appl. Pyrolysis* **2001b**, *58–59*, 387–400.

(18) Pakdel, H.; Vasile, C. L.; Roy, C. Chemical characterization of pyrolysis lignin from softwood vacuum pyrolysis. In *Proceedings of Science in Thermal and Chemical Biomass Conversion*; Bridgwater, A. V., Boocock, D. G. B., Eds.; CPL Press: Newbury, UK, 2006; 1189–1202.

(19) Bayerdach, R.; Nguyen, V. D.; Schurr, U.; Meier, D. *J. Anal. Appl. Pyrolysis* **2006**, *77*, 95–101.

(20) Garcia-Perez, M.; Chaala, A.; Pakdel, H.; Kretschmer, D.; Rodrigue, D.; Roy, C. *Energy Fuels* **2006**, *20*, 364–375.

(21) Garcia-Perez, M.; Chaala, A.; Pakdel, H.; Kretschmer, D.; Rodrigue, D.; Roy, C. *Energy Fuels* **2006**, *20*, 786–795.

(22) Czernik, S.; Johnson, D. K.; Black, S. *Biomass Bioenergy* **1994**, *7*, 187–192.

(23) Diebold, J. P.; Czernik, S. *Energy Fuels* **1997**, *11*, 1081–1091.

(24) Kawamoto, H.; Horigoshi, S.; Saka, S. *J. Wood Sci.* **2007**, *53*, 168–174.

(25) Meier, D.; Faix, O. *Bioresour. Technol.* **1999**, *68*, 71–77.

(26) Branca, C.; Giudicianni, P.; Di Blasi, C. *Ind. Eng. Chem. Res.* **2003**, *42*, 3190–3202.

(27) Garcia-Perez, M.; Chaala, A.; Pakdel, H.; Kretschmer, D.; Roy, C. *Biomass Bioenergy* **2007**, *31*, 222–242.

(28) Branca, C.; Di Blasi, C. *Ind. Eng. Chem. Res.* **2006**, *45*, 5891–5899.

(29) Li, C.-Z.; Wu, F.; Cai, H. Y.; Kandiyoti, R. *Energy Fuels* **1994**, *8*, 1039–1048.

(30) Peacocke, G. V. C.; Madrali, E. S.; Li, C.-Z.; Güell, A. J.; Wu, F.; Kandiyoti, R.; Bridgwater, A. V. *Biomass Bioenergy* **1994**, *7*, 155–167.

(31) Kershaw, J. R.; Sathe, C.; Hayashi, J.; Li, C.-Z.; Chiba, T. *Energy Fuels* **2000**, *14*, 476–482.

(32) Garcia-Perez, M.; Wang, S.; Shen, J.; Rhodes, M.; Tian, F.; Jin-Lee, W.; Hongwei, W.; Li, C.-Z. Fast Pyrolysis of Oil Mallee Woody Biomass: Effect of Temperature on the Yield and Quality of Pyrolysis Products. *Ind. Eng. Chem. Res.*, in press.

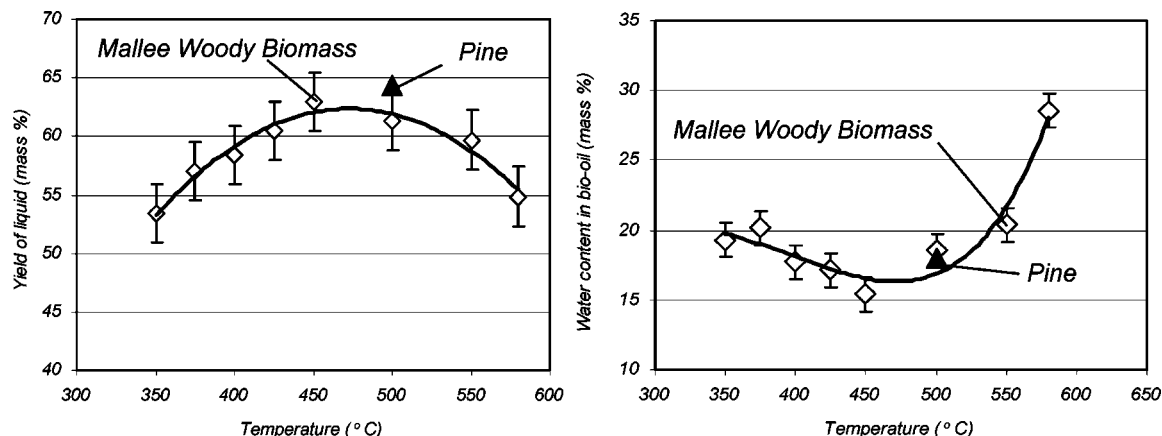


**Figure 1.** Yield of bio-oil and water concentration in bio-oil.

experimental error associated with these analyses. However, the filtration times also increased considerably to more than 3 h. The water-insoluble fraction was removed by filtration (Whatman 42, pore diameter 2.5  $\mu\text{m}$ ) and further quantified by weighing. The solid was washed with water and further extracted with dichloromethane until the filtrate was colorless. The remaining solid on the filter was dried at 105  $^{\circ}\text{C}$  for 1 h and was quantified as the water- $\text{CH}_2\text{Cl}_2$ -insoluble. The  $\text{CH}_2\text{Cl}_2$ -soluble fraction was rotary evaporated at 40  $^{\circ}\text{C}$  and quantified by weighing the resulting solid residue.

The thermogravimetric analysis of bio-oil was carried out by heating the bio-oil in nitrogen in a Perkin-Elmer Pyris 1 TGA. Between 5 and 10 mg of bio-oil sample was placed in a platinum crucible in the TGA. The test was started as soon as the bio-oil sample was added to the crucible to avoid the loss of the very light fractions in the flowing nitrogen used as the carrier gas. The sample was heated from 30 to 500  $^{\circ}\text{C}$  at a heating rate of 10  $^{\circ}\text{C}/\text{min}$ .

The analysis of bio-oil with GC-MS was carried out using a Hewlett-Packard GC-MS (HP6890 series GC with an HP5973 MS detector) with a capillary column (Agilent: HP-5MS, HP19091S-433) (length, 30 m; internal diameter, 250  $\mu\text{m}$ ; film thickness, 0.25  $\mu\text{m}$ ). The film in the column was formed of bonded 5% phenyl and 95% dimethyl polysiloxane. At least five standard solutions covering the concentration range in bio-oil samples were used to obtain the calibration curve for several of the compounds of interest. The response factor of each of the standards was calculated as the ratio between the gradients of their calibration curves and the one for the phenanthrene here used as internal standard. The following compounds were used for calibration: hydroxyacetaldehyde, acetic acid, acetol, propionic acid, cyclopentanone, 2-furaldehyde, furfuryl alcohol, 2-(5H)-furanone, phenol, *o*-cresol, eugenol, vanillin, levoglucosan, stilbene, and syringaldehyde. It was not possible to obtain standards for all the compounds identified in the GC/MS chromatograms. Consequently, the response factors for some compounds were considered equal to that for the standard of the closest chemical structure. Methanol solutions containing 4.5 mass % of bio-oil and 0.2 mass % of phenanthrene as the internal standard were used to quantify the chemical compounds of interest. The particles present in the bio-oil samples were removed with a microfilter (0.45  $\mu\text{m}$ ) prior to injection into the GC-MS. A 1  $\mu\text{L}$  sample was injected into the injection port set at 250  $^{\circ}\text{C}$  with a split ratio of 50:1. The injection syringe was washed with methanol both before and after each injection. The column was operated in a constant flow mode using 1 mL/min of helium as carrier gas. The column temperature was initially maintained at 40  $^{\circ}\text{C}$  for 1 min before increasing to 290  $^{\circ}\text{C}$  at a heating rate of 3  $^{\circ}\text{C}/\text{min}$ . A solvent delay of 2 min was employed. The mass spectrometer was operated at the electron ionization mode and scanned an  $m/z$  range of 32–500. The datum acquisition system was operated with the help of software G1034 C Chemstation with a NBS library. The identification of each compound was achieved based on retention time and the matching mass spectrum for the standard in the spectral library.

UV-fluorescence spectra were recorded at room temperature using a Perkin-Elmer LS50B spectrometer. The data were recorded

and analyzed with the FL Winlab software. Solutions of 4 ppm of bio-oil in methanol were prepared to avoid the effects of self-absorption. A quartz cell with a nominal 10 mm light pass-length and equipped with a PTFE lid was used. Preliminary tests were always carried out to verify that a linear relationship between the bio-oil concentration and its fluorescence intensity was achieved. The synchronous fluorescence spectra were recorded with a constant energy difference of  $-1400$  or  $-2800\text{ cm}^{-1}$  and a scan speed of 200 nm/min. Narrow emission and excitation monochromator slit widths of 2.5 nm were used to maximize selectivity. Each spectrum shown here represents the average of four scans.

### 3. Results and Discussion

**3.1. Bio-oil–Water Content.** Figure 1 presents the yield of oil and its content of water obtained from the pyrolysis of mallee woody biomass between 350 and 580  $^{\circ}\text{C}$  and pine at 500  $^{\circ}\text{C}$ . A maximum bio-oil yield was obtained at  $\sim 450$   $^{\circ}\text{C}$  from oil mallee.<sup>32</sup> The water content of bio-oil from mallee biomass, as determined with Karl Fisher titration, showed a minimum<sup>32</sup> at  $\sim 450$   $^{\circ}\text{C}$  at which the bio-oil yield peaked.

**3.2. GC-MS.** A typical total ion chromatogram of the bio-oil produced at 500  $^{\circ}\text{C}$  from mallee is presented in Figure 2. The retention times, the assignment to each peak, and the concentrations determined for each of the compounds are depicted in Table 1. The chemical compounds identified are mainly furans, phenols, carboxylic acids, alcohols, aldehydes, ketones, and sugars. It was possible to identify by GC-MS up to 34 mass % of the compounds present in the studied bio-oils. The compounds identified by GC-MS plus the water quantified by the Karl Fisher titration accounted for between 26 and 52 mass % of the oils. The most important organic species identified were acetic acid, hydroxypropanone, hydroxyacetaldehyde, and levoglucosan. The concentrations shown in Table 1 are very similar to those reported for other bio-oils in the literature.<sup>26</sup>

The concentrations presented in Table 1 multiplied by the corresponding overall bio-oil yields (Figure 1) gave the yields of individual species on the dry biomass basis as presented in Figure 3. The full content of this figure will be discussed throughout the rest of this paper. This figure shows the changes in the yields of the most important compounds as a function of pyrolysis temperature. It presents the yields of various chemical groups, including acetic acid (3.2–5.1 mass %), water (9.6–15.7 mass %), hydroxyacetaldehyde (0.6–3.0 mass %), levoglucosan (1.8–3.9 mass %), and hydroxypropanone (1.4–2.1 mass %) as well as the contents of phenols (1.2–4.0 mass %) and furans (0.97–1.8 mass %).

The yields of phenols and levoglucosan show a maximum at around 450–500  $^{\circ}\text{C}$ . The increases in the contents/yields of these



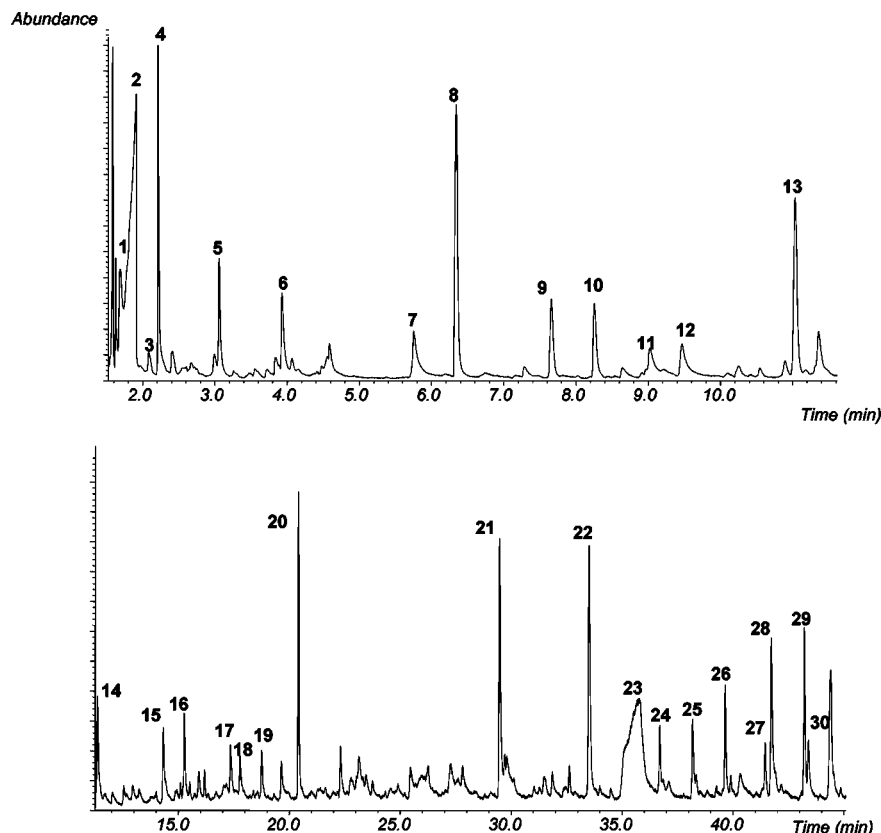


**Figure 2.** Total ion chromatogram obtained for the bio-oil produced at 500 °C. The retention times and the assignments to each peak are depicted in Table 1.

compounds with increasing pyrolysis temperature below 500 °C were a result of the intensification of the primary thermochemical reactions with temperature. The decreases in their yields at temperatures higher than 500 °C indicate that the rates of the secondary thermochemical decomposition reactions surpassed the rates of primary thermochemical reactions responsible for the formation of these compounds. The slight reduction in the yield of hydroxyacetaldehyde contrasts with that reported by Branca et al.<sup>26</sup> These differences could be attributed to differences in the feedstocks used, although the exact reasons remain a topic of further investigation.

### 3.3. Water-Insolubles by Precipitation in Cold Water.

Similarly, the content of water-insoluble fraction in the bio-oil multiplied by the corresponding yield of the bio-oil gives the yield of the water-insolubles, as is presented in Figure 3e. It is clear that a maximum yield of water-insolubles was observed at ~500 °C. It is noteworthy that most of the water-insoluble fraction consisted of compounds soluble in CH<sub>2</sub>Cl<sub>2</sub>, which are known to be small lignin-derived oligomers.<sup>27</sup> Previous studies have confirmed the presence of polyaromatics and extractive-derived compounds in this fraction in oils obtained from the vacuum pyrolysis of softwood bark<sup>33</sup> and from the Auger pyrolysis of pine.<sup>34</sup> However, the GC-MS analysis of the water-insoluble fraction did not show the presence of any of these compounds in the oils herein studied. In fact, the water-insolubles are believed to be responsible for the increases in bio-oil viscosity<sup>32</sup> with increasing pyrolysis temperature between 350 and 500 °C.

**3.4. Thermogravimetric Analysis.** The DTG curves for the bio-oils from the pyrolysis of mallee between 350 and 580 °C

are presented in Figure 4. Devolatilization of bio-oil in the TGA is a complex process combining the evaporation of light molecules and the cracking of heavy oligomers. The interpretation of the DTG curves was based on the hypothesis that compounds tend to behave independently and do not interact during evaporation and cracking. The compounds in bio-oils were classified into six families/groups.<sup>27</sup> Gaussian curves representative of independent groups of compounds were used to fit the curves. It was decided to use the Arrhenius dependence to describe both evaporation and cracking processes. The cracking equations have been commonly used for describing evaporation.<sup>27,28</sup> However, the interpretation of the resulting parameters requires special attention since they might not have the exact physical meanings as construed conventionally.

The values of activation energy ( $E_j$ ), pre-exponential factor ( $A_j$ ), order of reaction ( $n_j$ ), and the mass fraction of volatile materials ( $z_{j0}$ ) for each of the families were calculated from the DTG curves following a least-squares regression analysis. The number of “macro-families” adjusted depends upon the shape of the DTG curves. The parameters  $z_{j0}$  used to fit the thermogravimetric curves and the solid residue obtained are presented in Table 2.

The values of activation energies ( $E_j$ ) and reaction order ( $n_j$ ) were maintained constant to fit all the samples (see Table 3). Very small changes in the pre-exponential factors ( $A_j$ ) were needed to fit the curves (see Table 4). These changes in pre-exponential factors ( $A_j$ ) suggest a gradual change in the chemical composition within each family as the pyrolysis temperature increased. These changes could be linked to the deoxygenation of some organic molecules. The changes in the values of  $z_{j0}$  can be considered as a good indication of the variation in the content of the fraction itself.

Peak (family) A (Figure 3a) is assigned to the very volatile organic compounds, mainly hydroxyacetaldehyde, formic acid,

(33) Garcia-Perez, M.; Chaala, A.; Pakdel, H.; Kretschmer, D.; Roy, C. *J. Anal. Appl. Pyrolysis* **2007**, 78, 104–116.

(34) Garcia-Perez, M.; Adams, T. T.; Goodrum, J. W.; Geller, D. P.; Das, K. C. *Energy Fuels* **2007**, 21, 2363–2372.

Table 1. Composition of Bio-oil Determined by GC/MS (mass % of bio-oil)

no.	compd	family	RT (min)	temperature (°C)								pine pellets 500 °C
				350	375	400	425	450	500	550	580	
1	hydroxyacetaldehyde	A	1.6	4.63	4.84	3.88	3.57	4.84	3.71	1.10	4.51	
2	acetic acid	B	1.9	6.09	6.01	8.71	8.58	6.85	5.73	7.72	8.68	2.66
3	propane, 2,2 dimethoxy-	B	2.1	0.12	0.12	0.42	0.53	0.47	0.59	0.68	0.94	0.52
4	2-propanone, 1-hydroxy-(acetol)	B	2.3	2.65	3.09	3.21	2.71	3.03	2.16	2.80	3.84	3.55
5	propanoic acid	B	3.2	1.25	1.19	1.65	1.99	1.70	1.82	2.36	2.80	2.54
6	cyclopentanone	C	4.7	0.04	0.05	0.09	0.12	0.13	0.12	0.14	0.12	0.16
7	2-furaldehyde	C	5.9	0.21	0.55	0.48	0.49	0.38	0.33	0.41	0.59	0.41
8	furfuryl alcohol	C	7.0	0.05	0.06	0.05	0.04	0.04	0.02	0.03	0.04	0.03
9	furan, tetrahydro-2,5-dimethoxy- (cis)	C	7.8	0.24	0.36	0.56	0.54	0.30	0.34	0.45	0.33	0.22
10	furan, tetrahydro-2,5-dimethoxy- (trans)	C	8.4	0.19	0.32	0.45	0.45	0.25	0.29	0.35	0.28	0.18
11	2-(5H)-furanone	C	9.2	0.07	0.02	0.10	0.03	0.08	0.03	0.05	0.12	0.04
12	2-(5H)-furanone, 5-methyl-	C	9.7	0.12	0.11	0.11	0.19	0.11	0.07	0.02	0.06	0.05
13	2-furanethanol, $\beta$ -methoxy-	C	11.2	0.80	0.95	1.14	1.13	0.72	0.70	0.88	0.80	0.57
14	phenol	C	13.2	0.51	0.49	0.37	0.54	0.93	0.57	0.20	0.11	0.32
15	1,2-cyclopentanedione, 3-methyl-	C	14.7	0.03	0.05	0.07	0.08	0.05	0.04	0.02	0.02	0.01
16	phenol, 2-methyl-	C	16.1	0.06	0.07	0.07	0.07	0.05	0.05	0.04	0.06	0.03
17	phenol, 3-methyl- ( <i>o</i> -cresol)	C	16.4	0.02	0.01	0.02	0.02	0.01	0.02	0.02	0.02	
18	phenol, 2-methoxy- (guaiacol)	C	17.6	0.05	0.08	0.14	0.10	0.10	0.12	0.04	0.03	0.368
19	2-(3H)-furanone, dihydro-3-hydroxy-4,4-dimethyl-	C	19.0	0.09	0.05	0.12	0.11	0.08	0.07	0.04	0.02	0.04
20	phenol, 2-methoxy-4-methyl-	C	22.5	0.04	0.05	0.06	0.06	0.04	0.05	0.01	0.02	0.39
21	eugenol	C	29.8	0.36	0.41	0.58	0.57	0.46	0.51	0.26	0.26	0.21
22	vanillin	C	33.7	1.10	1.10	1.56	1.74	1.22	1.46	0.48	0.58	1.15
23	1,6-anhydro- $\beta$ -D-glucopyranose (levoglucosan)	D	35.4	3.39	3.41	5.86	6.33	4.73	6.49	5.79	3.46	6.32
24	hydroquinone	C	36.9	0.09	0.08	0.12	0.13	0.08	0.09	0.02	0.02	
25	stilbene	D	38.4	0.07	0.06	0.06	0.08	0.10	0.12	0.02	0.04	
26	phenol, 2,6 dimethoxy-4-(2-propenyl)-(cis) (4-propenyl syringol)	C	39.8	0.46	0.33	0.75	0.64	0.50	0.56	0.13	0.16	
27	phenol, 2,6 dimethoxy-4-(2-propenyl)-(trans) (4-propenylsyringol)	C	41.6	0.34	0.26	0.64	0.32	0.34	0.41	0.10	0.20	
28	syringaldehyde (benzaldehyde, 4-hydroxy-3,5 dimethoxy)	C	42.0	0.50	0.58	1.12	1.13	0.81	1.16	0.72	0.41	
29	propenoic acid, 3-(4-hydroxy-3-methoxyphenyl)-	C	43.4	1.34	1.22	1.43	1.21	1.00	0.99	0.11	0.25	
30	2,5-dimethoxy-4-ethylbenzaldehyde	C	43.6	0.24	0.07	0.17	0.25	0.26	0.31	0.07	0.06	
31	dibenzothiophene	D	44.6	0.12	0.08	0.15	0.15	0.12	0.17	0.08	0.07	0.05
	total			25.3	26.1	34.2	33.9	29.8	29.1	25.1	28.9	8.5

and methanol. Peak B (Figure 3b) is mainly due to water but also contains other organic compounds with boiling points close to water like acetic acid, acetol, and propionic acid. Phenols and furans are the main compounds in peak C (Figure 3c). Peak D (Figure 3d) is mainly due to sugars with a thermal behavior similar to that of levoglucosan. The bio-oils obtained by the vacuum pyrolysis of softwood bark<sup>33</sup> and by the auger pyrolysis of pine<sup>34</sup> also showed the presence of large contents of polyaromatics and extractive-derived compounds in fraction D. However, our GC-MS does not show the presence of any polyaromatics. Peak E (Figure 3e) was assigned mainly to oligomeric compounds insoluble in water but soluble in CH<sub>2</sub>Cl<sub>2</sub>.

The mechanism proposed to fit the DTG curves does not consider secondary char formation reactions, since the contribution of each family to the char formed cannot be measured. As a first approximation, it is supposed that all the char formed (see Figure 5) is due to the contribution of lignin-derived oligomers (family E, Figure 3e) and the oligosugars (family F, Figure 3f). The yield of char also showed a maximum at ~450 °C. This result is coherent with the larger peaks (Figure 4) corresponding to the lignin oligomers observed over the same range of pyrolysis temperatures. The oligomers (Families E and F) are likely to be the most important precursors of char formation.<sup>27</sup> Consequently, the content of each of the volatile fractions (A, B, C, and D) was estimated by multiplying  $z_{jo}$  (Table 2) by the content of the total volatiles. The content of

the total volatiles was determined as the difference between 100 and the solid residue ( $R_s$ ) (see values of  $R_s$  in Table 2). The contents of the oligomeric fractions (E and F) were estimated in the same way but their contributions to the formation of solid carbonaceous residues were taken into account by adding an additional term. This term was estimated by multiplying the value of  $R_s$  by the ratio between the volatile fraction of the family ( $z_{oi}$ ) and the total volatile fraction assigned to oligomers ( $z_{oE} + z_{oF}$ ).

Figure 6 shows the DTG curves of the water-insoluble—CH<sub>2</sub>Cl<sub>2</sub>-soluble fractions. The main peak of the water-insoluble—CH<sub>2</sub>Cl<sub>2</sub>-soluble fractions is clearly observed in the same region assigned to peak E. The presence of components represented by the peaks at low temperatures (e.g., <200 °C) is a reflection of the drawbacks of any solvent extraction techniques being unable to clearly separate the compounds (also see Introduction). It is clear that the volatilization/decomposition temperature of the main peak tended to shift to lower temperatures for oils produced at higher temperatures. This result is in agreement with the increases observed in the values of the pre-exponential factors for family E reported in Table 4. It is noteworthy that the peaks corresponding to the family E grow in the range of pyrolysis temperatures between 450 and 500 °C.

Peak F is usually found in the DTG curves of heavy but water-soluble fractions<sup>27</sup> and has been associated to oligomeric

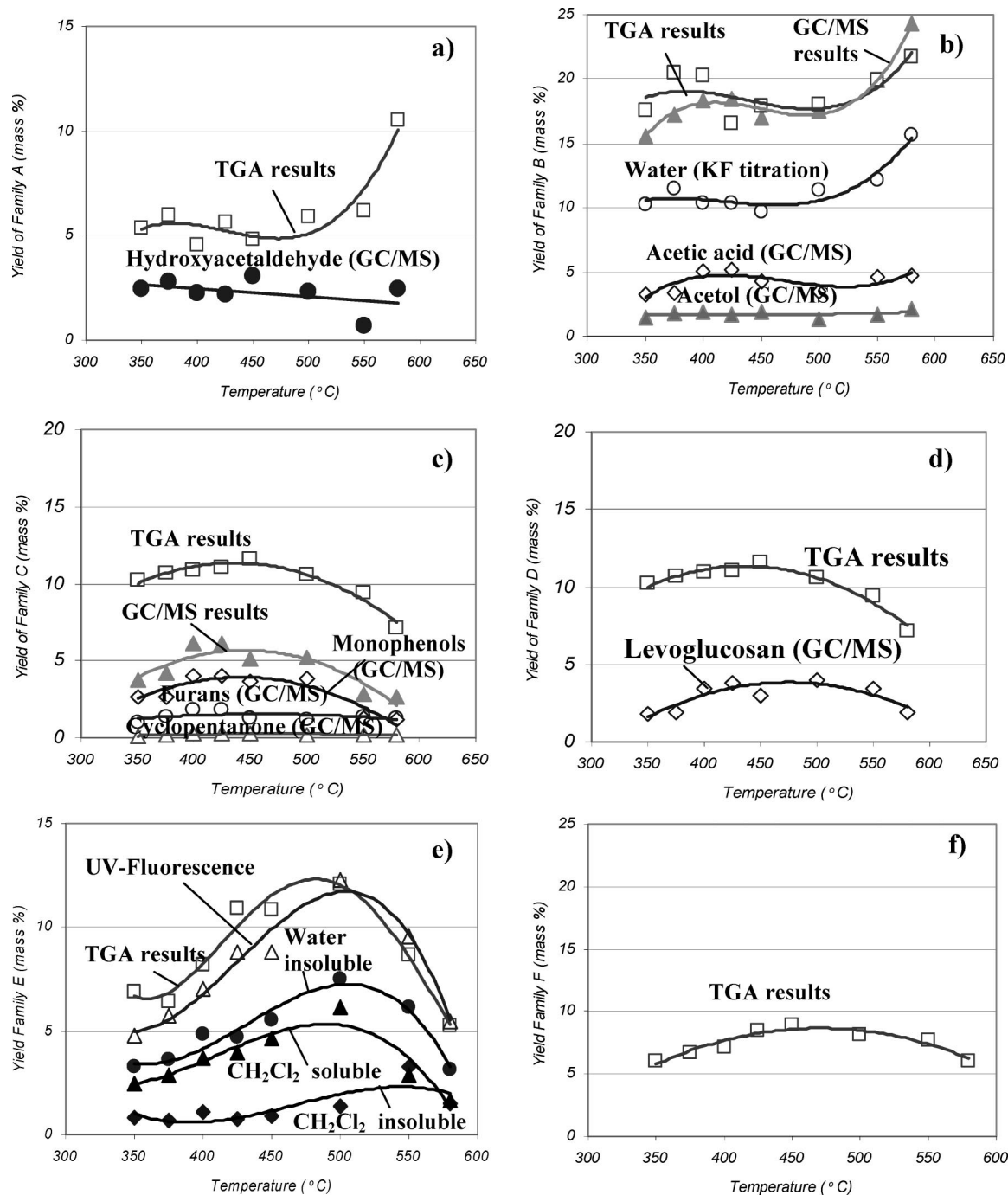


**Figure 3.** Yields of major chemical families (A, B, C, D, E, F) expressed as percentages of the initial biomass mass (on dry basis) as a function of pyrolysis reactor temperature.

compounds (e.g., oligosugars) soluble in water. More studies are needed to elucidate the chemical structure of these compounds.

Table 5 shows the content of each of the studied families as a function of temperature. All these values were multiplied by the yield of oil (Figure 1) to obtain the yield of each of the fractions on biomass dry basis (see Figure 3). The differences between the yield of family A and the yield of hydroxyacetaldehyde measured by GC-MS (Figure 3a) is due to formic acid, methanol, and ethanol which are important compounds but not measured by GC-MS in this study. A very good agreement was observed between the results obtained by GC-MS and Karl Fischer titration and those with TGA for family B (Figure 3b).

Conversely, the yields of family C determined by TGA were considerably larger than those determined by GC-MS (Figure 3c). This result is a clear indication of the existence of large

amounts of compounds with boiling points in the range between 100 and 250 °C that are not identified by the GC-MS method herein used. Similar differences were observed between the yields of family D determined by the GC-MS and TGA (Figure 3d). The yields determined by TGA were considerably larger than those determined by GC-MS for levoglucosan. Again, it is possible that several sugars with a thermal behavior similar to levoglucosan were not eluted by GC-MS.

The yields of family E determined by TGA (Figure 3e) were considerably larger than those of water-insolubles determined by the method of precipitation in cold water. A more detailed discussion of the causes for these large differences is presented in the next section. According to our TGA results, the fast pyrolysis of mallee woody biomass at 500 °C produced 23 mass % of organic monomers (families A, B, C) which could

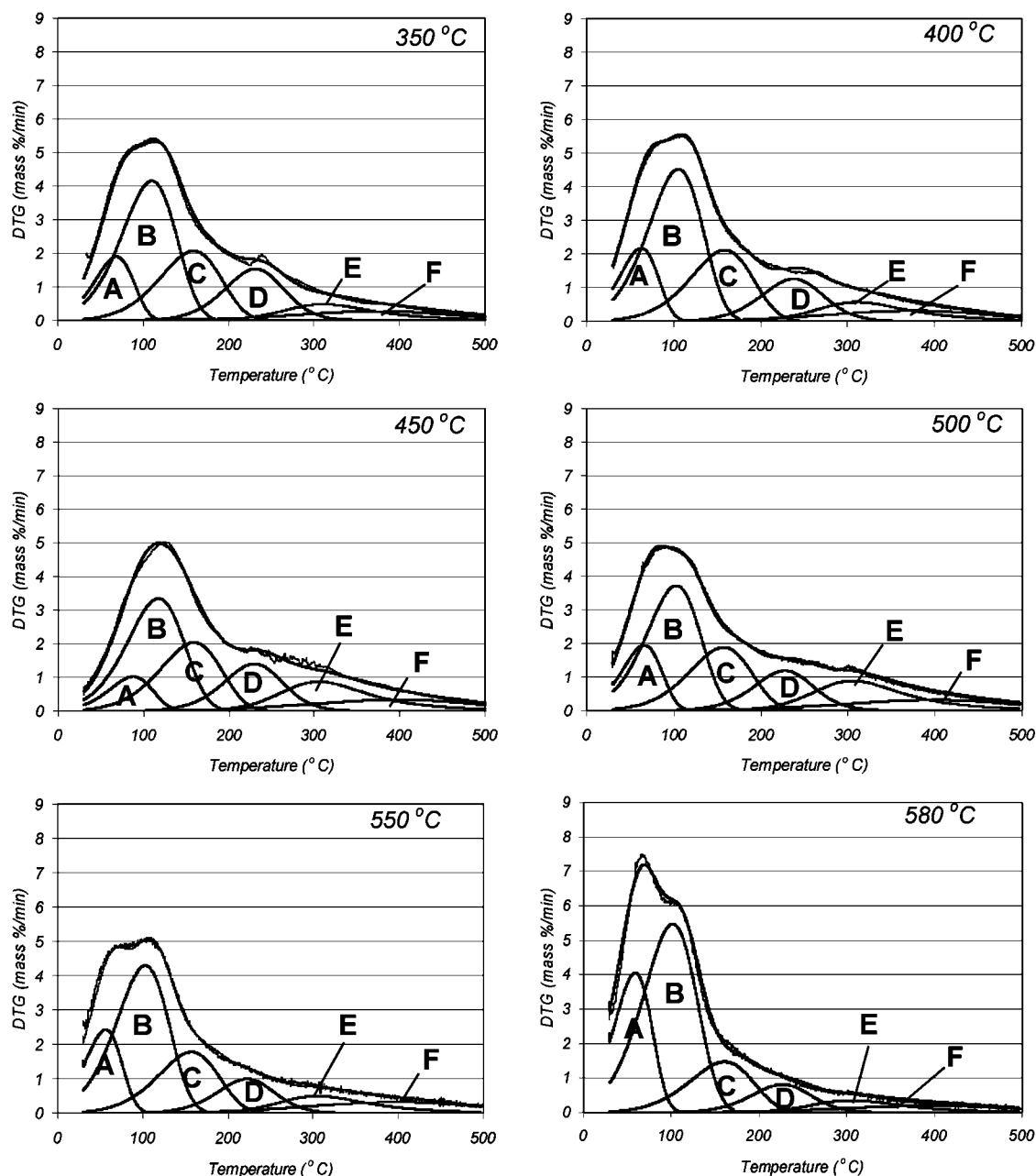


Figure 4. Deconvolution of DTG curves of bio-oils produced at different pyrolysis temperatures.

Table 2. Values of the Mass Fraction of Volatile Compounds and Solid Residue Used To Fit the DTG Curves

temp (°C)	mass fraction of volatiles $z_0$ (mass fraction)						solid residue ( $R_s$ ) (mass %)
	A	B	C	D	E	F	
350	0.11	0.38	0.21	0.15	0.08	0.07	10.96 ± 0.07
375	0.12 ± 0.01	0.40 ± 0.01	0.21	0.13 ± 0.01	0.07	0.07	11.15 ± 0.92
400	0.09 ± 0.03	0.39 ± 0.01	0.21	0.14 ± 0.01	0.09	0.08	11.43 ± 1.06
425	0.11 ± 0.01	0.32 ± 0.01	0.21 ± 0.01	0.15 ± 0.01	0.12 ± 0.03	0.09 ± 0.01	13.79 ± 1.65
450	0.08 ± 0.02	0.36 ± 0.04	0.23 ± 0.01	0.13 ± 0.02	0.11 ± 0.04	0.09 ± 0.01	14.14 ± 0.40
500	0.11 ± 0.06	0.35 ± 0.03	0.20 ± 0.02	0.12 ± 0.02	0.13 ± 0.01	0.09 ± 0.01	13.76 ± 1.01
550	0.12 ± 0.03	0.40 ± 0.01	0.19 ± 0.01	0.12 ± 0.04	0.08 ± 0.01	0.09	12.61 ± 0.76
580	0.21 ± 0.01	0.44 ± 0.02	0.14	0.09 ± 0.01	0.06 ± 0.01	0.06 ± 0.01	10.72 ± 1.38

Table 3. Values of Apparent Activation Energy and Reaction Order Used To Fit the DTG Curves

parameters	A	B	C	D	E	F
$E$ (kJ/mol)	39.8	35.2	40	67.9	81.6	32.6
$N$	1	1	1	1.4	2.5	1

potentially be stabilized to obtain transportation fuel additives. This yield is very similar to the yields of ethanol obtained from

the enzymatic hydrolysis of woody biomass.<sup>35</sup> Pyrolysis looks even more promising as a source for transportation fuels when considering the potential to ferment the sugars (families D and F) to produce more ethanol and to hydrotreat family E to produce aromatic hydrocarbons.

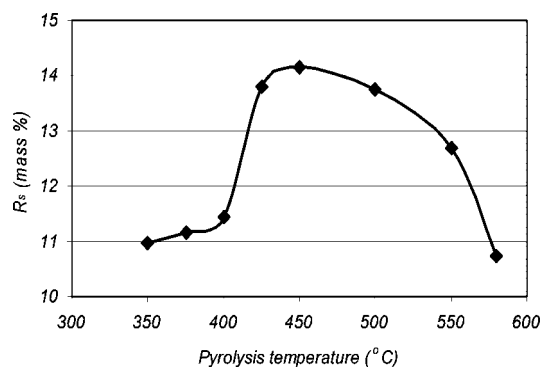
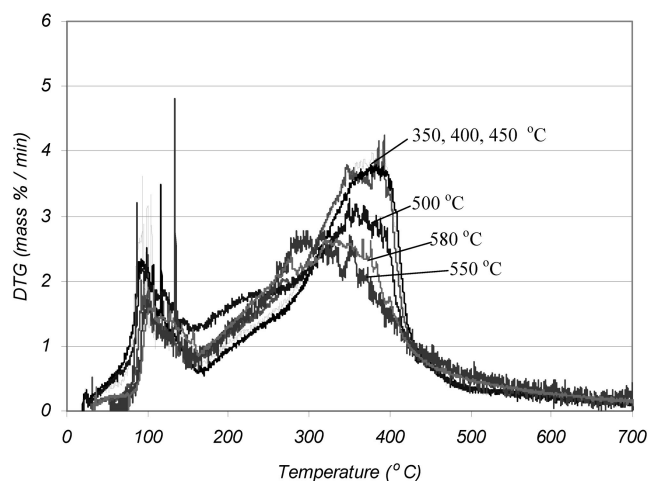
(35) Ithoh, H.; Wada, M.; Honda, Y.; Kuwahara, M.; Watanabe, T. *J. Biotechnol.* **2003**, *103* (3), 273–280.



**Table 4.** Values of Pre-exponential Factor Used To Fit the DTG Curves

temp (°C)	pre-exponential factor (A) (min <sup>-1</sup> )					
	A × 10 <sup>-5</sup>	B × 10 <sup>-4</sup>	C × 10 <sup>-4</sup>	D × 10 <sup>-6</sup>	E × 10 <sup>-6</sup>	F
350	4.7 ± 0.3	1.8	1.8	3.3	5.0	40
375	5.0 ± 1.6	1.8	1.8	2.6	3.0	40
400	4.8 ± 1.8	1.8 ± 0.3	1.8	2.6	5.0	40
425	6.6 ± 2.8	2.0 ± 0.4	1.8	3.2 ± 0.6	5.0	33 ± 7
450	5.0 ± 2.0	1.8 ± 0.2	1.7 ± 0.1	2.9 ± 0.6	6.0	30
500	4.5 ± 2.1	2.1 ± 0.2	1.8 ± 0.2	3.5 ± 0.5	6.0	30
550	6.5 ± 3.2	2.0 ± 0.5	1.9	4.6	6.0	30
580	5.9 ± 2.0	2.4 ± 0.2	1.8 ± 0.1	3.9	6.0	30

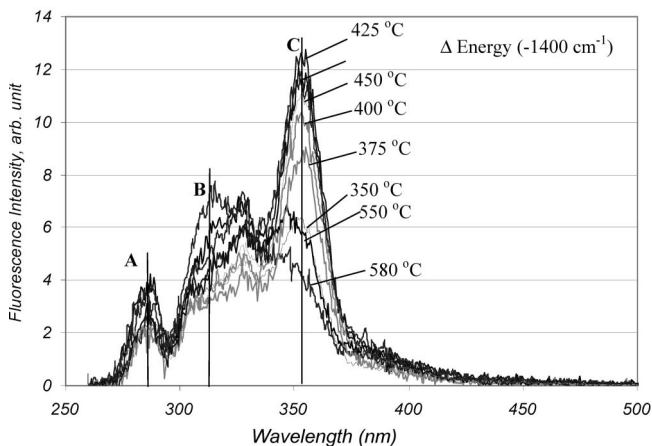
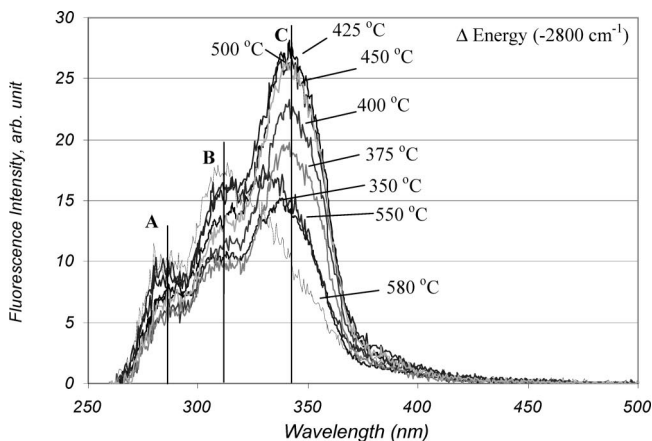
**3.5. UV-Fluorescence Spectroscopy.** Figure 7 presents the synchronous spectra of mallee bio-oils produced in the range of pyrolysis temperatures between 350 and 580 °C. The spectra were recorded using energy differences of  $-1400$  and  $-2800$  cm<sup>-1</sup>. The synchronous spectra of all the bio-oils showed three characteristic peaks centered at 270–280 nm (termed as peak A herein), 310–325 nm (termed as peak B) and 340–360 nm (termed as peak C). The peaks between 340 and 360 nm were always the most intense. The spectra recorded with  $\Delta\nu$  of  $-2800$  cm<sup>-1</sup> were always stronger than those with  $\Delta\nu$  of  $-1400$  cm<sup>-1</sup>, indicating the polar nature of the bio-oils, which tends to cause red shifts in fluorescence. However, both sets of spectra showed the same trends among different samples as shown in Figure 8. Peaks A and B tend to increase in intensity monotonically with increasing pyrolysis temperature, possibly implying increases in the concentrations of small aromatic ring systems (particularly those with one or two fused benzene rings) that form with

**Figure 5.** Solid residues of pyrolysis oils as a function of pyrolysis temperature.**Figure 6.** Thermogravimetric behavior of water-insoluble-CH<sub>2</sub>Cl<sub>2</sub>-soluble fractions of oils obtained at different temperatures.**Table 5.** Mass % of Each Family (A–F) Determined from the Mathematical Fitting of DTG Curves and the Mass Fraction of Solid Residue Determined Experimentally

temp (°C)	(% mass)					
	A	B	C	D	E	F
350	9.8	33.8	18.7	13.4	13.0	11.3
375	10.7	35.5	18.6	11.6	11.8	11.8
400	8.0	34.5	18.6	12.4	14.0	12.5
425	9.5	27.6	18.1	13.0	18.2	13.7
450	6.9	30.9	19.7	11.2	17.2	14.1
500	9.5	30.2	17.2	10.4	19.3	13.4
550	10.5	35.0	16.6	10.5	12.9	14.5
580	18.7	39.3	12.5	8.0	10.7	10.7

increasing pyrolysis temperature. Peak C appears to show a maximum at around 450–500 °C (Figure 8), coinciding with the maximum viscosity<sup>32</sup> and the maximum yield of oligomeric compounds that are water-insoluble but CH<sub>2</sub>Cl<sub>2</sub>-soluble (Figure 3e) over the same pyrolysis temperature range.

We then looked at the synchronous spectra for the water-insoluble-CH<sub>2</sub>Cl<sub>2</sub>-soluble fractions separated from bio-oils obtained from the pyrolysis of mallee between 350 and 580 °C. These spectra are presented in Figure 9. The spectra for this fraction only show two peaks centered at 310–325 and 340–360 nm. The gradual changes in the spectral shape are also in agreement with the changes in the shape of the DTG curves for the same fractions shown in Figure 6; both can be considered as a clear indication of changes in the chemical structure of these oligomers as a function of pyrolysis temperature. So, increases in pyrolysis temperature caused changes not only in the yield but also in the chemical structure of the oligomers.

**Figure 7.** Constant energy ( $-1400$  and  $-2800$  cm<sup>-1</sup>) synchronous spectra of bio-oils from the pyrolysis of Mallee oil biomass at different temperatures. The fluorescence intensity was recorded on the basis of the same bio-oil concentration 4 ppm.

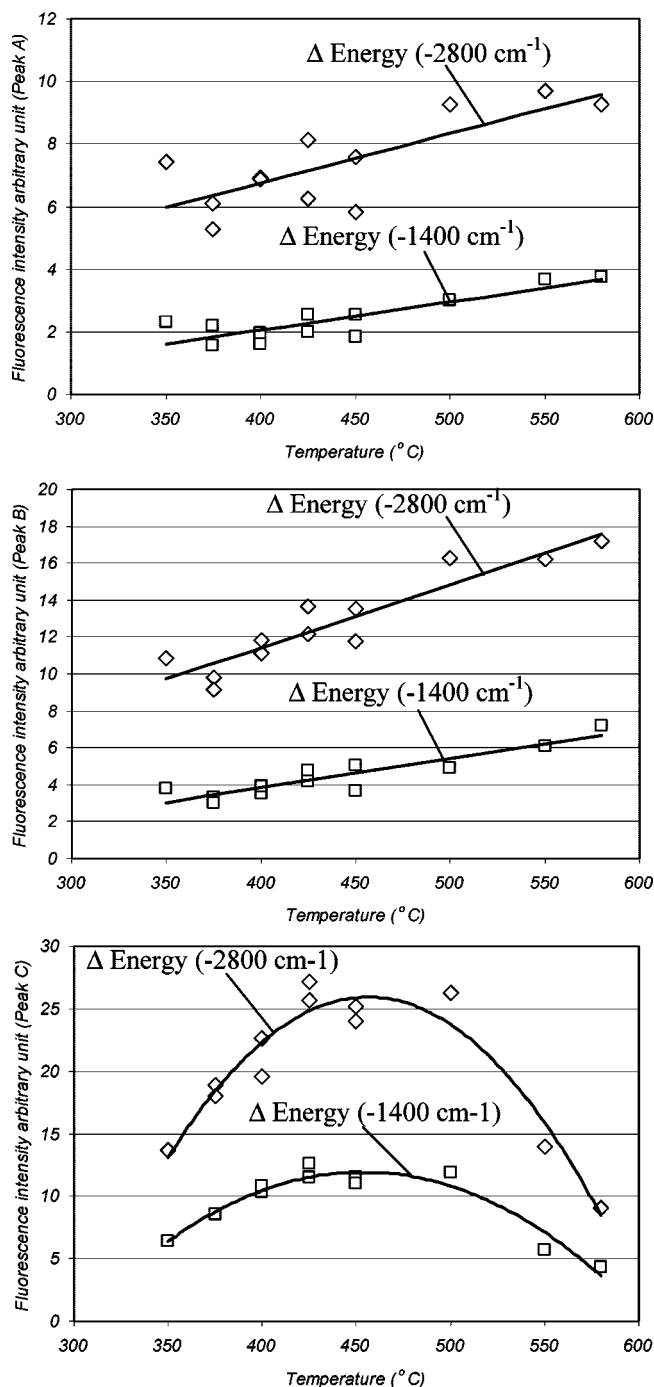


**Figure 8.** Intensity of main peaks identified in the synchronous spectra of bio-oils.

The separation of the water-insoluble- $\text{CH}_2\text{Cl}_2$ -soluble fractions from the raw bio-oils was purely a physical process. Therefore, it is reasonable to believe that the isolated water-insoluble- $\text{CH}_2\text{Cl}_2$ -soluble fractions have the same chemical structures as those in the original bio-oils. It is then possible to use the separated fractions as calibration “standards” for the synchronous spectrum. In this way, synchronous spectroscopy may be an alternative way to quantify the water-insoluble- $\text{CH}_2\text{Cl}_2$ -soluble materials in the raw bio-oils.

Since the synchronous spectral intensity showed a linear relationship with the concentration over the concentration range studied, the content of oligomers (i.e., water-insoluble but  $\text{CH}_2\text{Cl}_2$ -soluble) may be found as a factor so that multiplying the spectrum of the separated “standard” (water-insoluble- $\text{CH}_2\text{Cl}_2$ -soluble) with this factor should result in the spectrum of the

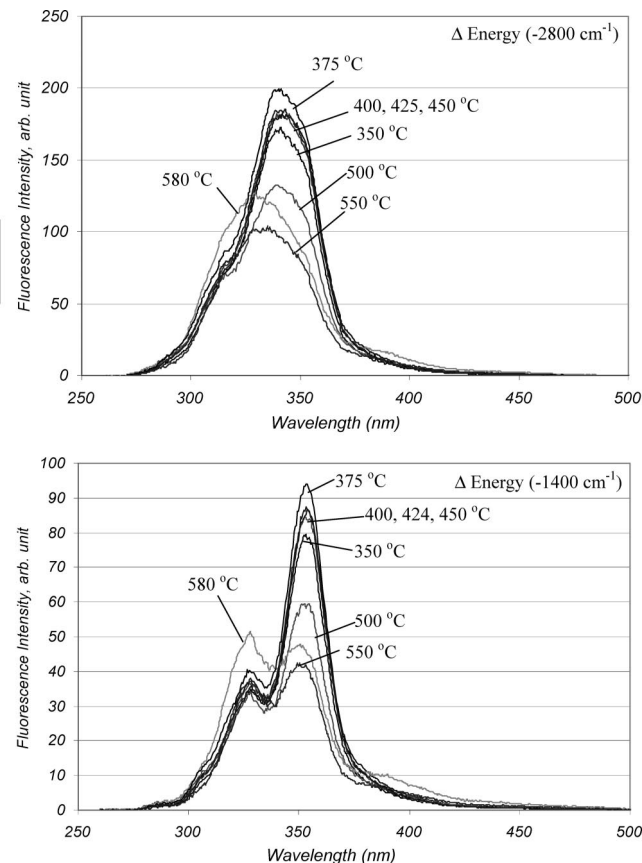


**Figure 9.** Constant energy ( $-1400$  and  $-2800\text{ cm}^{-1}$ ) synchronous spectra of water-insoluble- $\text{CH}_2\text{Cl}_2$ -soluble fractions from the pyrolysis of Mallee oil biomass at different temperatures. The fluorescence intensity was recorded on the basis of the same bio-oil concentration 4 ppm

raw bio-oil. It was initially thought that the right factor must be the yield of water-insoluble- $\text{CH}_2\text{Cl}_2$ -solubles determined by the precipitation in cold water. To our surprise, this factor gave a spectrum much weaker than that of the raw bio-oil (see Figure 10), indicating that the actual content of lignin-derived oligomers found in bio-oil must be considerably larger than that determined by the precipitation method. So it was decided to determine the factor by best fitting the spectra (higher wavelength portions) of the water-insoluble- $\text{CH}_2\text{Cl}_2$ -soluble fractions to the spectra of the raw (whole) oil. This approach proved to be successful as is shown in Figure 10. Short-wavelength parts ( $<330\text{ nm}$ ) of the spectra were not considered in the curve fitting because components other than oligomers contributed to these parts of the spectra. Figure 10 also shows that the above-mentioned curve-fitting method worked equally well for the bio-oil from the pyrolysis of pine.

The curve-fitting factors obtained were then multiplied by the yields of oils (Figure 1) to obtain the yields of the oligomers, as presented in Figure 3e. The presence of light compounds in the separated oligomeric fractions (as shown in Figure 6) could introduce errors when using these fractions as standards. We estimate that these light compounds could introduce errors between 5 and 10%. These errors could explain overestimations in the yields of oligomers of up to 1.2 mass % on biomass dry bases.

Good agreement was observed between the results obtained by TGA and those estimated by UV-fluorescence spectroscopy; both, however, showed important differences from those obtained by the cold water precipitation method. The differences can be explained by the existence of a certain amount of lignin-

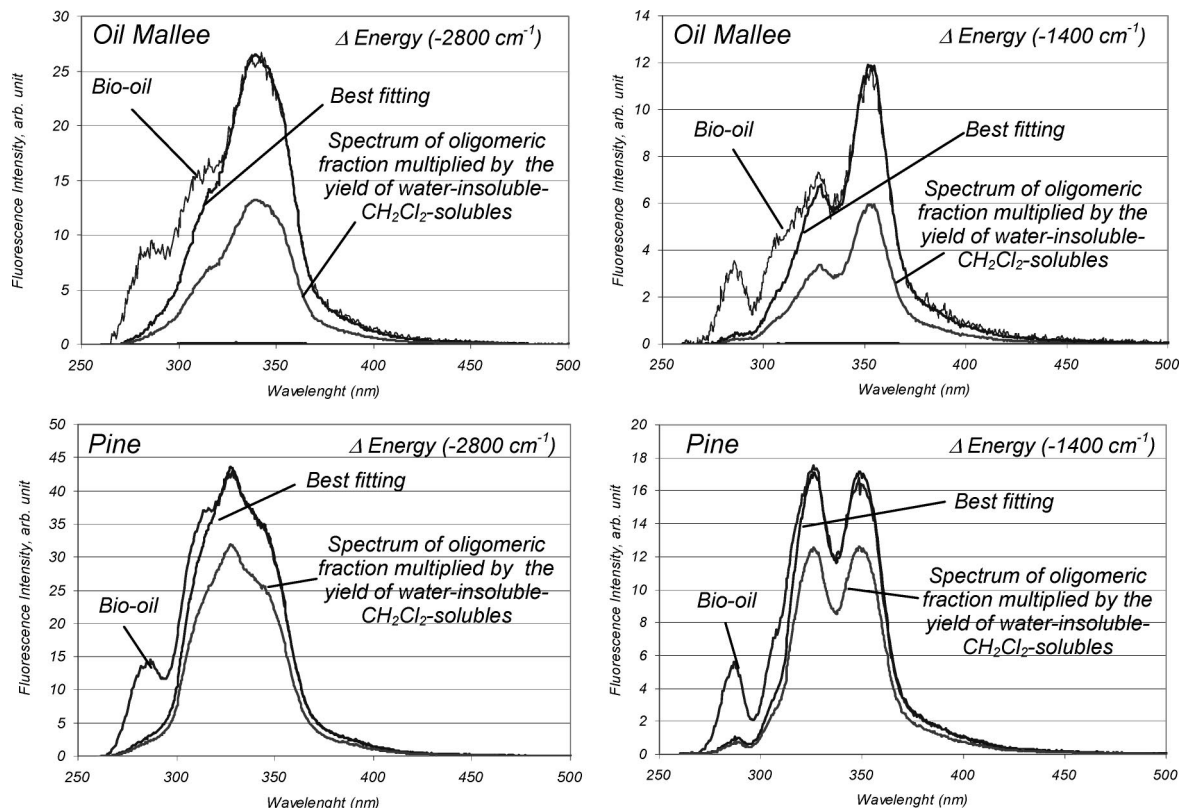


**Figure 10.** Fitting of UV-fluorescence spectra of whole bio-oil using the spectra recorded for the water-insoluble- $\text{CH}_2\text{Cl}_2$ -soluble fractions. Concentrations of 4 ppm.

derived oligomers that actually remain soluble in the water and do not precipitate to form a solid that can be filtered. In fact, further precipitation of solid from the water-soluble fractions was commonly observed two or three days after the initial precipitation in cold water and filtration. This suggests that an important amount of small and/or more polar lignin-derived oligomers might remain soluble in water in some metastable state or as suspended colloids. Clearly, these results demonstrate that the precipitation in cold water could seriously underestimate the content of oligomers in a bio-oil.

Figure 10 also shows that much weaker fluorescence emission was observed for the bio-oil derived from oil mallee than from pine at the same pyrolysis temperature of 500 °C. This difference can be attributed to differences in the structure of lignin-derived oligomers between hardwood (oil mallee) and softwood (pine).

Lignin is a heterogeneous aromatic polymer consisting of phenylpropane-units linked through various ether-types ( $\alpha$ - and  $\beta$ -ester) and condensed (C–C) types (aryl–aryl,  $\beta$ -aryl, and  $\beta$ - $\beta$ ) linkages.<sup>36</sup> Although, the ratio between each of these types of lignin changes depending of the species,  $\beta$ -ester is generally the most important linkage type. Kawamoto et al.<sup>24,37</sup> have studied the thermal degradation of different lignin dimer models and have proposed the existence of three mechanisms of reaction determining the composition and distribution of products during lignin pyrolysis. These mechanisms can be divided as (1)  $\text{C}_\beta$ –O cleavage (depolymerization) to yield monomers (cinnamyl alcohol and guaiacol), (2)  $\text{C}_\gamma$ -elimination (fragmentation) to form vinyl ethers and formaldehyde, and (3) condensation/carbonization reactions resulting in the formation of char.

GPC analyses of dioxane-soluble fractions obtained from the pyrolysis of lignin from Japanese cedar reported by Nakamura<sup>36</sup> also show a drastic increase in the yield of stilbene and lignin-derived oligomers between 350 and 400 °C. These GPC results confirm our findings that small oligomers with a relative narrow molecular weight distribution (under 1000 g/mol) are formed at temperatures over 350 °C.

The mechanism by which the oligomers are removed from the decomposing biomass is still unknown, but two hypotheses could be proposed. The first hypothesis could speculate about the existence of thermodynamically favorable conditions for the vaporization of dimers and trimers when molecules are formed from a solid at temperatures over 350 °C and at relatively low pressure. The second hypothesis considers that the thermodynamic conditions are not favorable for the evaporation of small oligomers, so the oligomers could be removed by mechanical entrainment generated by fast heating of biomass.<sup>12</sup> The fact that most of the oligomers observed were relatively small (soluble in  $\text{CH}_2\text{Cl}_2$ ) suggest the existence of a thermodynamically controlled process. In our opinion, mechanical entrainment cannot explain the existence of oligomers in such a narrow range of molecular weights.

#### 4. Conclusions

The evolution of the composition of bio-oil from the fast pyrolysis of oil mallee in a fluidized-bed reactor in the range of pyrolysis temperatures between 350 and 580 °C has been studied. The chemical composition of these oils was investigated using GC-MS, Karl Fischer titration, solvent extraction (including precipitation in cold water), thermogravimetry, and constant energy synchronous fluorescence spectroscopy. The content of lignin-derived oligomers obtained by TGA was found to be very similar to that estimated by UV-fluorescence spectroscopy but

(36) Nakamura, T.; Kawamoto, H.; Saka, S. Pyrolysis behavior of Japanese cedar wood lignin studied with various model dimers. *J. Anal. Appl. Pyrolysis*, in press.

(37) Kawamoto, H.; Horigoshi, S.; Saka, S. *J. Wood Sci.* **2007**, 53, 268–271.

was considerably larger than the one determined by precipitation in cold water. This result suggests that a relatively large amount of small and/or more polar lignin-derived oligomers remain (metastably) soluble in cold water, limiting the use of cold-water precipitation as a method to determine the oligomer content. Our results indicate the existence of a maximum in the yield of lignin-derived oligomers between 450 and 500 °C. In fact, most of the increase in the yield of bio-oil observed between 350 and 500 °C can be explained by the formation of this fraction.

**Acknowledgment.** The authors are very thankful to the Australian Research Council (ARC Discovery Grant DP0556098) for the financial support of this project. This project also received funding from the Australian Government as part of the Asia-Pacific Partnership on Clean Development and Climate. The authors also thank Mr. Rick Giles of the Revegetation Unit, Department of Conservation and Lands, Western Australia, for kindly providing the biomass used.

EF7007634